Crystal structures and electronic properties of $UTi_xNb_{3-x}O_{10}$ ($x=0,1/3,1$) and of the intercalation compound $Li_{0.9}UTiNb_2O_{10}$

Peter G. Dickens,* Gavin J. Flynn, Saban Patat and Gary P. Stuttart

Inorganic Chemistry Laboratory, South Parks Road, Oxford, UK OX1 3QR

Complete crystal structures of the related phases $UTi_xNb_{3-x}O_{10}$ ($x=0,1/3,1$) and of the intercalation compound $Li_{0.9}UTiNb_2O_{10}$ have been determined by Rietveld analysis of room-temperature powder neutron diffraction data. The new structural data combined with magnetic susceptibility measurements made in the range $5<T/K<300$ support a common electronic formulation of the compounds as $Li^{I}_{y}U^{V}_{1+y-x}U^{VI}_{x-y}Ti^{IV}_{x}Nb^{V}_{3-x}O_{10}$ ($y\leqslant x\leqslant 1$) with $U^{V}(f^1)$ being the only paramagnetic species present.

UV_3O_{10},[1] UNb_3O_{10}[2] and $UTi_xNb_{3-x}O_{10}$[3] belong to a family of isostructural mixed oxides of uranium having pillared-layer structures based on edge- and vertex-sharing of UO_8 and MO_6 polyhedra in which edge-shared UO_6 hexagons and MO_4 rectangles form extended planar arrays linked together by metal–oxygen chains running perpendicular to them. The common interlayer chain sequence is U–O–M_{II}–O–M_I–O–M_{II}–O–U, where the transition-metal atoms M occupy two different crystallographic sites. The characteristic interlayer separation is *ca.* 4 Å and the repeat distance along the chain direction *ca.* 16 Å. Each uranium atom is thus surrounded by a hexagonal-bipyramidal array of oxygen atoms, the two axial oxygens above and below the plane being much closer to the uranium than are the six planar oxygens. The oxygen atom arrangement around the metal M is approximately octahedral for both M_I and M_{II}, but an off-centre distortion in the chain direction is associated with M_{II}. A plan of the structure, which is orthorhombic, viewed along the [001] chain direction, and based on the coordinates for UV_3O_{10},[1] is shown in Fig. 1. Only for this phase have accurate oxygen positions been determined by neutron diffraction. An early single-crystal study of UNb_3O_{10} by Chevalier and Gasperin[2] placed the heavy-metal positions satisfactorily, but large temperature factors together with a poor *R* value (0.1) suggested that significant uncertainty in the positions of the oxygen atoms remained.

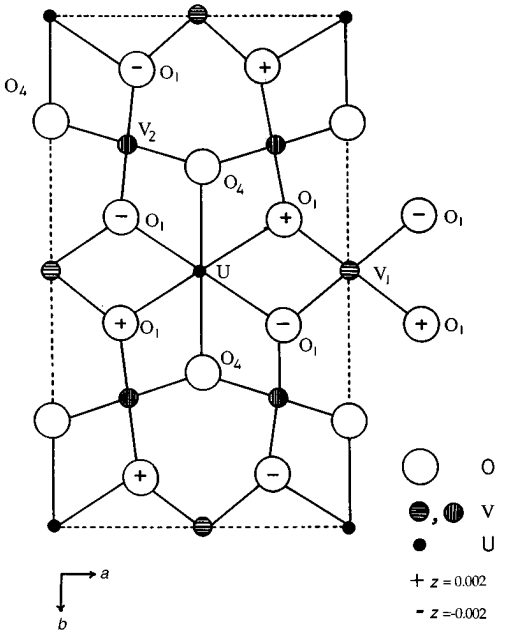

Fig. 1 Structure of UV_3O_{10} in the ***ab*** plane ($z=0$)

These authors suggested, on the basis of the metal–oxygen vectors associated with each metal site, that $Nb^{IV}(d^1)$ and Nb^{V} occupied the M_I and M_{II} sites, respectively, with uranium present exclusively as U^{VI}. This valence assignment conflicts, however, with the electronic structure of UNb_3O_{10} determined by magnetic and PES measurements by Miyake and co-workers[4] which identified U^{V} (f^1) and not $Nb^{IV}(d^1)$ as the paramagnetic centre in stoichiometric UNb_3O_{10}, suggesting a formulation of the compound as $U^{V}Nb^{V}{}_3O_{10}$. This electronic arrangement makes better chemical sense since the equilibrium oxygen pressure at 300 K, calculated from tabulated thermodynamic data,[5,6] for a NbO_2–Nb_2O_5 mixture is very much lower than that for a UO_3–U_3O_8 (or even U_3O_8–U_4O_9) couple, and hence spontaneous conversion of Nb^{IV} to Nb^{V} and U^{VI} to U^{V} in a solid solution of the oxides is the likely outcome. A further single-crystal X-ray study on '$UTiNb_2O_{10}$' (having the actual composition $UTi_{1/3}Nb_{8/3}O_{10}$) by Chevalier and Gasperin[3] led to the conclusion that this solid-solution phase also had the UNb_3O_{10}-type structure with ($Ti^{IV}{}_{1/3}$, $Nb^{IV}{}_{2/3}$) occupying the M_I site, Nb^{V} the M_{II} site, and uranium again present as U^{VI}. In order to determine the light atom positions accurately, and thus establish the precise oxygen environments of the metal atom sites, we report herein structure determinations, by powder neutron diffraction, of the compounds UNb_3O_{10}, $UTi_{1/3}Nb_{8/3}O_{10}$ and $UTiNb_2O_{10}$; for the last compound no crystal structure has been reported previously. In addition, new magnetic susceptibility measurements have been made which enable changes in electronic behaviour to be associated with changes in metal environments and thus assist in the identification of the species responsible for the observed paramagnetism in this series of related compounds. The stoichiometric compound $UTiNb_2O_{10}$ contains all metal atoms in their highest oxidation states and, like other oxides and mixed oxides[7] containing U^{VI} in tunnelled or layered structures, undergoes intercalation reactions at ambient temperatures in which small electropositive elements, such as lithium, are incorporated interstitially with retention of the parent oxide structure. We report below a determination, by powder neutron diffraction, of the complete crystal structure of one such compound, $Li_{0.9}UTiNb_2O_{10}$, for which the changes in electronic properties caused by intercalation have been monitored by magnetic susceptibility measurements. This work is part of an ongoing investigation of the structural and electronic properties of intercalation compounds formed by the oxides and mixed oxides of uranium.

Experimental

Preparations

The starting materials used for making samples of the mixed oxides were AnalaR-grade Nb_2O_5 and TiO_2 and synthetic

U_3O_8 and NbO_2. U_3O_8 was prepared by decomposition of $UO_4 \cdot 2H_2O$[8] as described previously.[9] NbO_2 was made by reduction of Nb_2O_5 in a stream of dry hydrogen at 1273 K; its composition and structural identity were confirmed by thermogravimetry and its powder X-ray pattern.[10] Three members of the U–Nb–Ti–O system were prepared according to reactions (1)–(3):

$$1/3NbO_2 + 1/3U_3O_8 + 4/3Nb_2O_5 \rightarrow UNb_3O_{10} \quad (1)$$

$$Nb_2O_5 + TiO_2 + 1/3U_3O_8 + 1/6O_2 \rightarrow UTiNb_2O_{10} \quad (2)$$

$$4/3Nb_2O_5 + 1/3TiO_2 + 1/3U_3O_8 \rightarrow UTi_{1/3}Nb_{8/3}O_{10} \quad (3)$$

The starting mixtures for reactions (1) and (3) were ground, pelletised and heated in evacuated sealed silica tubes for 24 h at 1373 K. To ensure complete reaction the products were reground, repelletised and reheated in the absence of air. UNb_3O_{10} was dark brown and its powder X-ray pattern was consistent with that reported by Kovba *et al.*[11] $UTi_{1/3}Nb_{8/3}O_{10}$ was also brown and its X-ray pattern was readily indexable on an orthorhombic cell of similar lattice parameters to those reported by Chevalier and Gasperin.[3] The starting mixture for reaction (2) was finely ground, pelletised and heated in an open alumina boat at 1373 K; after regrinding, repelletising and reheating a yellow single-phase product resulted whose X-ray diffraction pattern (Table 1) closely resembled those of $UTi_{1/3}Nb_{8/3}O_{10}$ and UNb_3O_{10}.

The intercalation compounds $Li_{0.90}UTiNb_2O_{10}$ and $Li_{0.34}UTiNb_2O_{10}$ were prepared at ambient temperature in an inert atmosphere by adding Bu^nLi to the parent oxide in dried hexane. The procedures used followed closely those employed previously for the preparation (and the subsequent chemical characterisation by redox titration) of other uranium oxide intercalation compounds.[12] The crystallinity of the products was enhanced by prolonged annealing at 473 K. The indexed powder diffraction pattern of $Li_{0.9}UTiNb_2O_{10}$, which was used for further structural investigations, is given in Table 2.

Table 1 Powder X-ray diffraction data for $UTiNb_2O_{10}$ ($\lambda = 1.54056$ Å)[a]

$2\theta_{obs}$/degrees	d_{obs}/Å	intensity	index	d_{calc}/Å
15.011	5.897	m	111	5.892
17.684	5.011	m	022	5.011
21.417	4.146	vw	113	4.146
21.487	4.132	s	004	4.125
25.021	3.556	w	131	3.556
26.739	3.331	w	202	3.332
28.282	3.153	vs	040	3.154
29.397	3.036	m	133	3.036
30.552	2.924	vw	115	2.924
35.833	2.504	s	224	2.506
38.123	2.359	m	151	2.360
39.327	2.289	m	242	2.290
40.766	2.211	m	117	2.208
41.234	2.188	m	313	2.187
43.817	2.064	m	008	2.063
45.858	1.977	w	137	1.979
46.178	1.964	w	333	1.964
46.984	1.932	vw	155	1.933
50.050	1.821	m	260	1.821
50.647	1.801	w	246	1.801
53.026	1.725	m	228	1.726
53.486	1.712	vw	422	1.711
54.717	1.676	vw	317	1.676
55.087	1.666	w	264	1.666
55.084	1.666	m	404	1.666
57.651	1.598	vw	02 10	1.596
58.447	1.578	m	080	1.577
61.658	1.503	vw	20 10	1.503
63.047	1.473	m	084	1.473
63.739	1.459	vw	11 11	1.459
65.406	1.426	vw	282	1.425
66.541	1.404	vw	177	1.405
67.477	1.387	vw	13 11	1.387
68.721	1.365	m	268	1.365

[a]Refined orthorhombic cell parameters: $a = 7.283(2)$ Å, $b = 12.616(2)$ Å, $c = 16.501(2)$ Å.

Powder neutron diffraction data

UNb_3O_{10}. Data were collected at room temperature on the instrument D2B at ILL, Grenoble, from a 10 g sample contained in a thin-walled vanadium can using a neutron wavelength of 1.5946 Å. The standard Rietveld method for constant wavelength data refinement was used in the Brookhaven National Laboratories version[13] and its application followed in all important respects that described by us recently for the structure refinement of $USbO_5$.[14] The starting structural parameters chosen for refinement of UNb_3O_{10} were those given by Chevalier and Gasperin[2] from single-crystal data. Refinement proceeded smoothly for data in the range $15 < \theta/\text{degrees} < 145$ and the final cycle included 25 variables and converged with the following R values:[14] $R_1 = 6.8$, $R_{wp} = 7.9$, $R_p = 5.9$, $R_E = 1.7\%$. Cell and positional parameters are given in Table 3 and selected interatomic distances and bond angles in Table 4. The profile fit is shown in Fig. 2. An attempt to improve the refinement by removal of symmetry constraints through transformation to $P\bar{1}$ led to no significant improvement in the goodness of fit or to changes of atom positions from those found for the original orthorhombic (*Fddd*) space group.

Table 2 Powder X-ray diffraction data for $Li_{0.9}UTiNb_2O_{10}$[a]

$2\theta_{obs}$/degrees	d_{obs}/Å	intensity	index	d_{calc}/Å
14.979	5.909	m	111	5.916
17.754	4.991	m	022	5.000
21.598	4.111	m	113	4.115
21.950	4.046	s	004	4.050
24.889	3.574	m	131	3.579
26.634	3.344	m	202	3.342
28.077	3.175	vs	040	3.178
29.432	3.032	m	133	3.035
30.955	2.886	vw	115	2.886
35.911	2.499	s	224	2.500
37.846	2.375	m	151	2.376
39.101	2.302	m	242	2.303
41.081	2.195	m	313	2.194
41.498	2.174	m	117	2.174
44.618	2.029	m	008	2.025
45.969	1.972	w	333	1.972
46.480	1.952	w	137	1.957
47.047	1.930	w	155	1.930
49.652	1.834	s	260	1.835
50.845	1.794	w	246	1.795
53.640	1.707	m	228	1.708
54.879	1.672	m	264	1.671
57.986	1.589	m	080	1.589
62.755	1.479	m	084	1.479
68.989	1.360	m	268	1.360

[a]Refined orthorhombic cell parameters: $a = 7.338(5)$ Å, $b = 12.712(4)$ Å, $c = 16.199(7)$ Å.

Table 3 Unit-cell and positional parameters for UNb_3O_{10}[a]

	site	x	y	z	B/Å^2
U	8a	1/8	1/8	1/8	0.63(4)
Nb_1	8b	1/8	1/8	5/8	0.73(5)
Nb_2	16g	1/8	1/8	0.3836(1)	0.60(3)
O_1	32h	0.4279(2)	0.2261(2)	0.1231(2)	0.84(5)
O_2	16g	1/8	1/8	0.5004(2)	1.20(4)
O_3	16g	1/8	1/8	0.2438(2)	1.15(4)
O_4	16f	1/8	0.3267(3)	1/8	0.90(9)

[a]Cell parameters: $a = 7.4173(3)$ Å, $b = 12.8418(5)$ Å, $c = 15.8269(3)$ Å; $Z = 8$; space group *Fddd*.

Table 4 Selected bond lengths (Å) and angles (degrees) in UNb_3O_{10}

U—O_1 (×4)	2.595(2)	Nb_1—O_1 (×4)	1.955(1)	Nb_2—O_1 (×2)	1.960(1)
U—O_3 (×2)	1.880(1)	Nb_1—O_2 (×2)	1.972(2)	Nb_2—O_2	1.848(2)
U—O_4 (×2)	2.590(1)	Nb_2—O_4 (×2)	1.960(2)	Nb_2—O_3	2.213(2)

O_1^{i}—U—O_1^{ii}	60.0(3)	O_1^{vii}—Nb_1—O_2^{i}(O_1^{viii}—Nb_1—O_2^{ii})	90.9(3)
O_1^{ii}—U—O_1^{iv}(O_1^{i}—U—O_1^{iii})	178.7(2)	O_1^{vii}—Nb_1—O_2^{ii}(O_1^{viii}—Nb_1—O_2^{i})	89.1(3)
O_1^{i}—U—O_3^{i}	90.7(2)	O_1^{v}—Nb_2—O_1^{vi}	170.3(2)
O_1^{i}—U—O_3^{ii}	89.3(2)	O_1^{v}—Nb_2—O_2^{i}	94.9(2)
O_1^{i}—U—O_4^{i}(O_1^{iii}—U—O_4^{ii})	60.0(5)	O_1^{v}—Nb_2—O_3^{ii}	85.1(2)
O_3^{i}—U—O_3^{ii}	180	O_1^{v}—Nb_2—O_4^{iv}(O_1^{vi}—Nb_2—O_4^{iii})	82.8(2)
O_4^{i}—U—O_3^{i}	90	O_1^{v}—Nb_2—O_4^{iii}(O_1^{vi}—Nb_2—O_4^{iv})	96.5(3)
O_1^{vii}—Nb_1—O_1^{viii}	83.2(4)	O_2^{i}—Nb_2—O_4^{iii}	94.0(3)
O_1^{vii}—Nb_1—O_1^{x}	96.8(4)	O_3^{ii}—Nb_2—O_4^{iii}	86.0(3)
O_1^{vii}—Nb_1—O_1^{ix}(O_1^{viii}—Nb_1—O_1^{x})	178.2(7)	O_4^{iii}—Nb_2—O_4^{iv}	172.0(3)

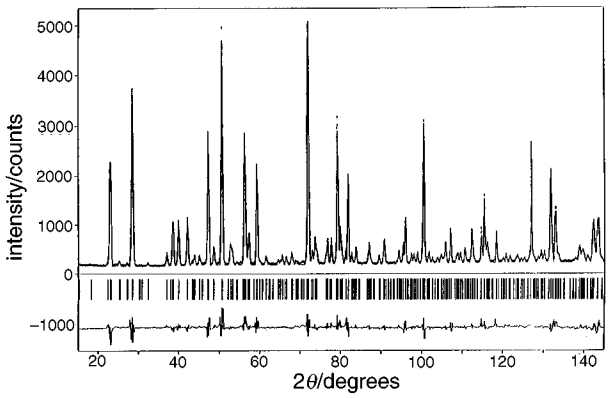

Fig. 2 Observed (points), calculated (line) and difference (lower line) profiles for UNb_3O_{10}

$UTi_xNb_{3-x}O_{10}$. Neutron time-of-flight data for the two oxides $UTi_{1/3}Nb_{8/3}O_{10}$ and $UTiNb_2O_{10}$ were collected at room temperature from powder samples (*ca.* 10 g) contained in thin-walled vanadium cans using the medium resolution high-intensity POLARIS diffractometer at ISIS. The details of data handling, manipulation and display, and the model refinement programs used were the same as those described by us in recently published structure determinations of $U_2V_2O_{11}$ and UV_2O_8.[15] For members of the $UTi_xNb_{3-x}O_{10}$ family of compounds the starting model adopted for refinement of both data sets was that proposed by Chevalier and Gasperin[3] for $UTi_{1/3}Nb_{8/3}O_{10}$. In space group *Fddd*, 8 (Ti_xNb_{1-x}) units were placed at M_I sites (8b) and 16 Nb at M_{II} sites (16 g). For these partially ordered arrangements the refinements progressed smoothly but converged with poor *R* values,[16] $R_I \approx 11$ and $R_{wp} \approx 8\%$, and unreasonable temperature factors for titanium and niobium. It became clear that Ti should not be restricted to an exclusive occupation of the M_I sites. Hence, the trial model was modified by distributing Ti evenly between the (8b) and (16 g) sites in the statistical ratio of 1 : 2. The refinements improved dramatically and the final cycle was extended to incorporate the site occupancies as additional variables subject only to the constraints of correct overall stoichiometry and complete occupancy of each Ti/Nb site. The final *R* values were satisfactory for both compounds: $UTi_{1/3}Nb_{8/3}O_{10}$: $R_I = 5.5$, $R_{wp} = 3.7$, $R_p = 4.1$, $R_E = 1.7\%$; $UTiNb_2O_{10}$: $R_I = 8.0$, $R_{wp} = 4.7$, $R_p = 5.9$, $R_E = 1.5\%$.

Unit-cell parameters, atomic positions and principal bond lengths and angles are summarised in Tables 5–8. In $UTi_{1/3}Nb_{8/3}O_{10}$ the refined site occupancies confirm that titanium is disordered randomly over both niobium sites. In $UTiNb_2O_{10}$ there is apparently a small preference for titanium to occupy the M_I sites, which may be a real effect or merely an artefact of the level of refinement achieved.

$Li_{0.9}UTiNb_2O_{10}$. Powder neutron diffraction data for $Li_{0.9}UTiNb_2O_{10}$ were collected at room temperature on the POLARIS diffractometer. Refinement proceeded initially by including only atoms of the parent oxide framework and taking the atomic coordinates listed in Table 7 as a starting model. This continued to a final cycle incorporating 39 variables which converged with the following *R* values: $R_I = 9.4$, $R_{wp} = 4.2$, $R_p = 5.7$. Difference Fourier maps based on observed and calculated structure factors were synthesised for sections in the interlayer region ($z \approx 0.25$) and the strongest negative peak was observed at *ca.* (0,0.2,0.23). Lithium was sited at this position with an occupancy of 0.25. This led to improvement in the profile fit and allowed the positional, thermal and site occupancy parameters for lithium to be incorporated into the final refinement culminating in a satisfactory profile fit and the following *R* values: $R_I = 7.1$, $R_{wp} = 3.8$, $R_p = 4.9$, $R_E = 0.6\%$.

Structural parameters are given in Table 9 and bond lengths and angles in Table 10. The site occupancy of the lithium refined to a value (0.24) which was consistent with the extent of insertion ($x = 0.9$) determined by redox titration and no additional lithium was located in the structure.

Magnetic measurements

Magnetic susceptibilities of pure phases of $UTi_xNb_{3-x}O_{10}$ ($x = 0$, 0.34, 0.90, 1.0) were measured over the temperature range 5–300 K and at field strengths 0.1–1 T using a model S600C SQUID susceptometer (Cryogenic Ltd.). Raw values were corrected for atomic diamagnetic contributions and the data converted to molar susceptibilities, $\chi_m(T)$. In the range 150–300 K the susceptibilities of all the compounds followed

Table 5 Unit-cell and positional parameters for $UTi_{1/3}Nb_{8/3}O_{10}$[a]

	site	*x*	*y*	*z*	B/Å^2	occupancy
U	8a	1/8	1/8	1/8	0.73(4)	
Ti_1/Nb_1	8b	1/8	1/8	5/8	1.45(9)	0.111(9)/0.889(9)
Ti_2/Nb_2	16g	1/8	1/8	0.3894(1)	0.72(4)	0.111(4)/0.889(4)
O_1	32h	0.4275(3)	0.2262(2)	0.1216(2)	0.75(4)	
O_2	16g	1/8	1/8	0.5009(2)	1.07(3)	
O_3	16g	1/8	1/8	0.2416(2)	1.03(6)	
O_4	16f	1/8	0.3263(2)	1/8	0.27(5)	

[a]Cell parameters: $a = 7.3554(5)$ Å, $b = 12.7218(9)$ Å, $c = 15.949(1)$ Å; $Z = 8$; space group *Fddd*.

Table 6 Selected bond lengths (Å) and angles (degrees) in $UTi_{1/3}Nb_{8/3}O_{10}$

U—O_1 (×4)	2.572(1)	$Nb_1(Ti_1)$—O_1 (×4)	1.939(1)	$Nb_2(Ti_2)$—O_1 (×2)	1.954(1)
U—O_3 (×2)	1.861(1)	$Nb_1(Ti_1)$—O_2 (×2)	1.983(2)	$Nb_2(Ti_2)$—O_2	1.776(2)
U—O_4 (×2)	2.557(1)	$Nb_2(Ti_2)$—O_4 (×2)	1.955(1)	$Nb_2(Ti_2)$—O_3	2.355(1)

O_1^{i}—U—O_1^{ii}	60.2(2)	O_1^{vii}—$Nb_1(Ti_1)$—O_2^{i} [O_1^{viii}—$Nb_1(Ti_1)$—O_2^{ii}]	91.6(1)
O_1^{ii}—U—O_1^{iv}(O_1^{i}—U—O_1^{iii})	177.6(1)	O_1^{vii}—$Nb_1(Ti_1)$—O_2^{ii} [O_1^{viii}—$Nb_1(Ti_1)$—O_2^{i}]	88.4(1)
O_1^{i}—U—O_3^{i}	91.2(2)	O_1^{v}—$Nb_2(Ti_2)$—O_1^{vi}	163.3(2)
O_1^{i}—U—O_3^{ii}	88.8(2)	O_1^{v}—$Nb_2(Ti_2)$—O_2^{i}	98.3(2)
O_1^{i}—U—O_4^{i}(O_1^{iii}—U—O_4^{ii})	60.0(1)	O_1^{v}—$Nb_2(Ti_2)$—O_3^{ii}	81.7(2)
O_3^{i}—U—O_3^{ii}	180	O_1^{v}—$Nb_2(Ti_2)$—O_4^{iv} [O_1^{vi}—$Nb_2(Ti_2)$—O_4^{iii}]	82.0(2)
O_4^{i}—U—O_3^{i}	90	O_1^{v}—$Nb_2(Ti_2)$—O_4^{iii} [O_1^{vi}—$Nb_2(Ti_2)$—O_4^{iv}]	96.0(2)
O_1^{vii}—Nb_1—O_1^{viii}	83.1(1)	O_2^{i}—$Nb_2(Ti_2)$—O_4^{iii}	96.7(1)
O_1^{vii}—Nb_1—O_1^{x}	97.0(1)	O_3^{ii}—$Nb_2(Ti_2)$—O_4^{iii}	83.3(1)
O_1^{vii}—$Nb_1(Ti_1)$—O_1^{ix} [O_1^{viii}—$Nb_1(Ti_1)$—O_1^{x}]	176.8(2)	O_4^{iii}—$Nb_2(Ti_2)$—O_4^{iv}	166.6(2)

Table 7 Unit-cell and positional parameters for $UTiNb_2O_{10}$[a]

	site	*x*	*y*	*z*	*B*/Å²	occupancy
U	8a	1/8	1/8	1/8	0.98(7)	
Ti_1/Nb_1	8b	1/8	1/8	5/8	0.6(2)	0.40(1)/0.60(1)
Ti_2/Nb_2	16g	1/8	1/8	0.3980(3)	0.61(8)	0.302(6)/0.698(6)
O_1	32h	0.4232(4)	0.2257(3)	0.1233(3)	0.85(5)	
O_2	16g	1/8	1/8	0.5059(2)	1.04(5)	
O_3	16g	1/8	1/8	0.2337(2)	1.16(6)	
O_4	16f	1/8	0.3295(4)	1/8	0.56(8)	

[a]Cell parameters: $a = 7.2511(5)$ Å, $b = 12.5628(9)$ Å, $c = 16.448(1)$ Å; $Z = 8$; space group *Fddd*.

Table 8 Selected bond lengths (Å) and angles (degrees) in $UTiNb_2O_{10}$

U—O_1 (×4)	2.506(2)	$Nb_1(Ti_1)$—O_1 (×4)	1.935(1)	$Nb_2(Ti_2)$—O_1 (×2)	1.950(2)
U—O_3 (×2)	1.788(1)	$Nb_1(Ti_1)$—O_2 (×2)	1.959(2)	$Nb_2(Ti_2)$—O_2	1.775(2)
U—O_4 (×2)	2.570(2)	$Nb_2(Ti_2)$—O_4 (×2)	1.938(1)	$Nb_2(Ti_2)$—O_3	2.702(2)

O_1^{i}—U—O_1^{ii}	60.7(1)	O_1^{vii}—$Nb_1(Ti_1)$—O_2^{i} [O_1^{viii}—$Nb_1(Ti_1)$—O_2^{ii}]	90.8(1)
O_1^{ii}—U—O_1^{iv}(O_1^{i}—U—O_1^{iii})	178.7(2)	O_1^{vii}—$Nb_1(Ti_1)$—O_2^{ii} [O_1^{viii}—$Nb_1(Ti_1)$—O_2^{i}]	89.2(1)
O_1^{i}—U—O_3^{i}	90.7(1)	O_1^{v}—$Nb_2(Ti_2)$—O_1^{vi}	156.0(2)
O_1^{i}—U—O_3^{ii}	89.3(1)	O_1^{v}—$Nb_2(Ti_2)$—O_2^{i}	102.0(1)
O_1^{i}—U—O_4^{i}(O_1^{iii}—U—O_4^{ii})	59.7(1)	O_1^{v}—$Nb_2(Ti_2)$—O_3^{ii}	78.0(2)
O_3^{i}—U—O_3^{ii}	180	O_1^{v}—$Nb_2(Ti_2)$—O_4^{iv} [O_1^{vi}—$Nb_2(Ti_2)$—O_4^{iii}]	81.0(1)
O_4^{i}—U—O_3^{i}	90	O_1^{v}—Nb_2—O_4^{iii} [O_1^{vi}—$Nb_2(Ti_2)$—O_4^{iv}]	94.3(1)
O_1^{vii}—$Nb_1(Ti_1)$—O_1^{viii}	81.7(2)	O_2^{i}—$Nb_2(Ti_2)$—O_4^{iii}	101.2(1)
O_1^{vii}—$Nb_1(Ti_1)$—O_1^{x}	98.3(1)	O_3^{ii}—$Nb_2(Ti_2)$—O_4^{iii}	78.8(1)
O_1^{vii}—$Nb_1(Ti_1)$—O_1^{ix}[O_1^{viii}—$Nb_1(Ti_1)$—O_1^{x}]	178.3(2)	O_4^{iii}—$Nb_2(Ti_2)$—O_4^{iv}	157.5(1)

Table 9 Unit-cell and positional parameters for $Li_{0.9}UTiNb_2O_{10}$[a]

	site	*x*	*y*	*z*	*B*/Å²	occupancy
U	8a	1/8	1/8	1/8	1.76(5)	
Ti_1/Nb_1	8b	1/8	1/8	5/8	1.0(1)	0.383(8)/0.617(8)
Ti_2/Nb_2	16g	1/8	1/8	0.3924(2)	0.43(5)	0.308(4)/0.692(4)
O_1	32h	0.4275(3)	0.2268(2)	0.1211(1)	1.06(4)	
O_2	16g	1/8	1/8	0.5012(2)	1.40(3)	
O_3	16g	1/8	1/8	0.2450(2)	1.93(5)	
O_4	16f	1/8	0.3263(2)	1/8	0.96(6)	
Li	32h	0.903(2)	0.191(2)	0.249(1)	0.77(3)	0.24(2)

[a]Cell parameters: $a = 7.3563(2)$ Å, $b = 12.7162(3)$ Å, $c = 16.1997(4)$ Å; $Z = 8$; space group *Fddd*.

the Langevin–Debye relationship: $\chi_m = C/T + A$, where C is the Curie constant and A a temperature-independent paramagnetic term. Plots of χ_m *vs.* T and χ_m^{-1} *vs.* T for UNb_3O_{10} are shown in Fig. 3 and plots of χ_m *vs.* T for the intercalation compounds $Li_yUTiNb_2O_{10}$ ($y = 0,0.34,0.90$) are shown in Fig. 4. The quantities C and A derived from these data are shown in Table 11 together with the corresponding effective magnetic moments, μ_{eff}. This last quantity is defined through the expression $\mu_{eff}/\mu_B = (3kC/N_A\mu_B^2\mu_0 n)^{1/2}$, where n is the number of paramagnetic centres in a formula unit, identified as $1-x$ in

Table 10 Selected bond lengths (Å) and angles (degrees) in $Li_{0.9}UTiNb_2O_{10}$

$U-O_1$ (×4)	2.575(1)	$Nb_2(Ti_2)-O_4$ (×2)	1.961(1)	$Li-O_1$	2.088(4)
$U-O_3$ (×2)	1.945(2)	$Nb_2(Ti_2)-O_1$ (×2)	1.955(2)	$Li-O_2$	2.206(3)
$U-O_4$ (×2)	2.560(1)	$Nb_2(Ti_2)-O_2$	1.763(1)	$Li-O_3$	1.841(3)
$Nb_1(Ti_1)-O_1$ (×4)	1.946(2)	$Nb_2(Ti_2)-O_3$	2.387(2)	$Li-O_{3'}$	2.352(5)
$Nb_1(Ti_1)-O_2$ (×2)	2.006(2)			$Li-O_4$	2.058(4)

$O_1^{i}-U-O_1^{ii}$	60.4(2)	$O_1^{vii}-Nb_1(Ti_1)-O_2^{i}$ $[O_1^{viii}-Nb_1(Ti_1)-O_2^{ii}]$	91.8(1)
$O_1^{ii}-U-O_1^{iv}(O_1^{i}-U-O_1^{iii})$	177.2(2)	$O_1^{vii}-Nb_1(Ti_1)-O_2^{ii}$ $[O_1^{viii}-Nb_1(Ti_1)-O_2^{i}]$	88.2(1)
$O_1^{i}-U-O_3^{i}$	91.4(1)	$O_1^{v}-Nb_2(Ti_2)-O_1^{vi}$	159.7(2)
$O_1^{i}-U-O_3^{ii}$	88.6(1)	$O_1^{v}-Nb_2(Ti_2)-O_2^{i}$	100.1(2)
$O_1^{i}-U-O_4^{i}(O_1^{iii}-U-O_4^{ii})$	59.8(2)	$O_1^{v}-Nb_2(Ti_2)-O_3^{ii}$	79.9(2)
$O_3^{i}-U-O_3^{ii}$	180	$O_1^{v}-Nb_2(Ti_2)-O_4^{iv}$ $[O_1^{vi}-Nb_2(Ti_2)-O_4^{iii}]$	81.7(1)
$O_4^{i}-U-O_3^{i}$	90	$O_1^{v}-Nb_2-O_4^{iii}$ $[O_1^{vi}-Nb_2(Ti_2)-O_4^{iv}]$	95.4(1)
$O_1^{vii}-Nb_1(Ti_1)-O_1^{viii}$	83.4(2)	$O_2^{i}-Nb_2(Ti_2)-O_4^{iii}$	98.3(2)
$O_1^{vii}-Nb_1(Ti_1)-O_1^{x}$	96.7(1)	$O_3^{ii}-Nb_2(Ti_2)-O_4^{iii}$	81.7(2)
$O_1^{vii}-Nb_1(Ti_1)-O_1^{ix}[O_1^{viii}-Nb_1(Ti_1)-O_1^{x}]$	176.3(3)	$O_4^{iii}-Nb_2(Ti_2)-O_4^{iv}$	163.5(3)
O_1-Li-O_2	79.6(5)	$O_2-Li-O_{3'}$	107.4(7)
O_1-Li-O_3	108.4(7)	O_2-Li-O_4	82.7(5)
$O_1-Li-O_{3'}$	78.2(4)	$O_3-Li-O_{3'}$	122.1(7)
O_1-Li-O_4	156.9(7)	O_3-Li-O_4	94.4(6)
O_2-Li-O_3	130.5(6)	$O_{3'}-Li-O_4$	93.4(6)

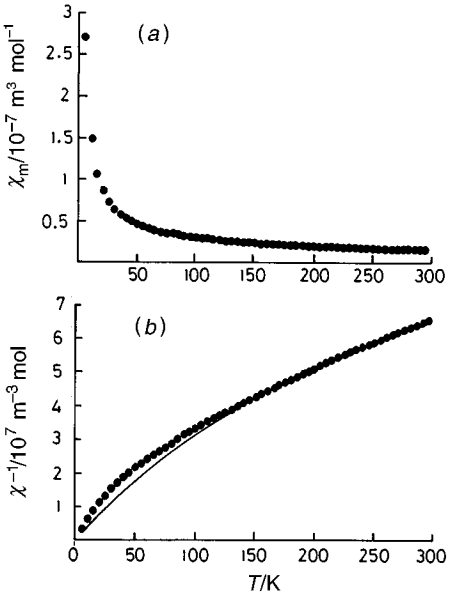

Fig. 3 (*a*) χ_m *vs.* *T* for UNb_3O_{10}. (*b*) $\chi_m{}^{-1}$ *vs.* *T* for UNb_3O_{10}: ●, measured; —, calculated.

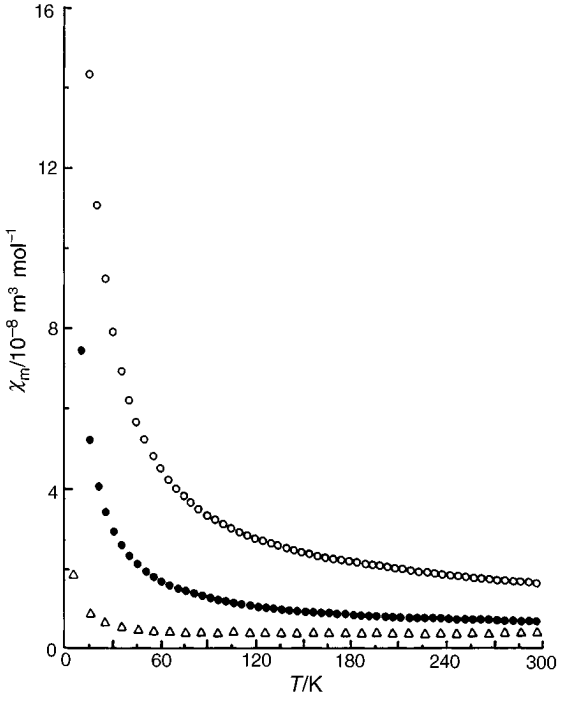

Fig. 4 χ_m *vs.* *T* for $Li_yUTiNb_2O_{10}$: △, $y=0$; ●, $y=0.34$; ○, $y=0.90$

$UTi_xNb_{3-x}O_{10}$ and *y* in $Li_yUTiNb_2O_{10}$. *C* and the standard physical constants used in this equation are expressed in SI units.

Discussion

$UTi_xNb_{3-x}O_{10}$

The structure of UNb_3O_{10} determined by the present powder neutron diffraction study is shown in Fig. 5(*a*); in Fig. 5(*b*) the atomic arrangements about the three metal sites U, M_I (Nb_1) and M_{II} (Nb_2), which are members of a chain running parallel to the ***c*** axis, are shown in greater detail. The gross features of the structure agree with those deduced by Chevalier and Gasperin[2] from X-ray data but significant differences in metal–oxygen distances are found (Table 4) which have consequences for the interpretation of electronic structures for this and for the other $UTi_xNb_{3-x}O_{10}$ phases examined. The local environment about uranium in each phase is hexagonal bipyramidal with shorter axial and longer equatorial U—O bonds present.

Table 11 Magnetic data for UNb_3O_{10} and $Li_yUTiNb_2O_{10}$

compound	*T*/K	$C/10^{-9}$ m^3 mol^{-1} K	$A/10^{-11}$ m^3 mol^{-1}	μ_{eff}/μ_B
UNb_3O_{10}	150–300	2500	698	1.26
$Li_{0.34}UTiNb_2O_{10}$	200–300	672	780	1.12
$Li_{0.90}UTiNb_2O_{10}$	200–300	2395	688	1.30

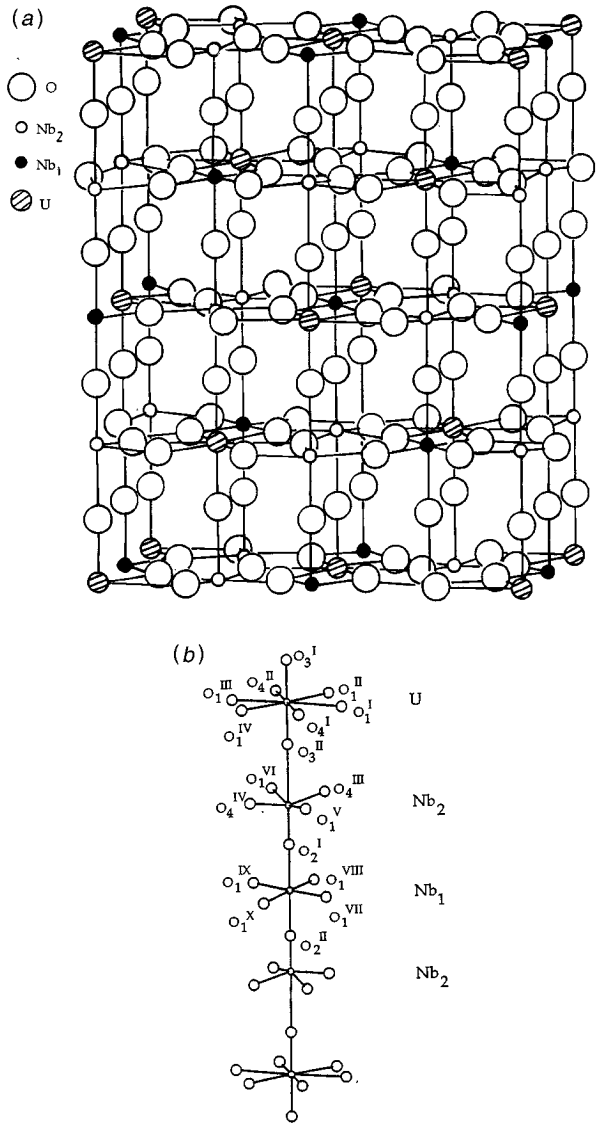

Fig. 5 (*a*) Structure of UNb_3O_{10}; (*b*) chain parallel to *c* in UNb_3O_{10} (numbering of oxygen atoms refers to Table 3)

The observed changes in U—O bond lengths along the sequence $x=0$, 1/3, 1.0 are summarised in Table 12. The shortening observed in the axial and equatorial U—O bond lengths on passing from UNb_3O_{10} to the fully oxidised $UTiNb_2O_{10}$ suggests electron removal from uranium occurs when Ti is substituted for Nb. The calculated bond-valence sums[17] for uranium, v_U, based on the new structural data, quantify this progressive trend and imply that oxidation of U^V to U^{VI} occurs in this sequence. From the data provided in Tables 4–8 Nb_1 is found to be at the centre of a nearly regular octahedron of oxygens for UNb_3O_{10} and the same environment occurs for Nb_1/Ti_1 in the titanium substituted oxides with Nb_1/Ti_1—O bonds falling in a narrow range of 1.93–1.98 Å. In contrast the environment about the M_{II} site, either Nb_2 in UNb_3O_{10} or Nb_2/Ti_2 in the titanium-substituted oxides, approximates to a square-pyramidal arrangement with significantly different axial Nb—O distances occurring; for example, in UNb_3O_{10} the values found are: $Nb_2-O_2=1.848$ (1.95 Å) and $Nb_2-O_3=2.213$ (2.17) Å. This is a not uncommon arrangement for Nb^V which occurs, for example, in $KNbO_3$ (and is also found for Ti^{IV} in $BaTiO_3$). However, an important result, guiding the interpretation of electronic structure, is that the bond-valence sums about Nb_1 and Nb_2 in UNb_3O_{10}, calculated using the new bond-length data and atomic parameters tabulated by Altermatt and Brown,[17] are virtually identical at 5.2 and 5.1 respectively, and correspond to a common oxidation state (v) for Nb; this implies the correct electronic formulation for the unsubstituted oxide is $U^VNb^V{}_3O_{10}$. This assignment contradicts the conclusion of Chevalier and Gasperin[2,3] who suggested that Nb^{IV} was present (at the M_I site), but supports the results of Miyake *et al.*[4] who showed by XPS measurements that oxidation of UNb_3O_{10} to UNb_3O_{10+x} was accompanied by the removal of electrons from uranium and not from niobium. In addition the magnetic measurements made in the present work (Fig. 3) show that UNb_3O_{10} behaves as a dilute paramagnet having, in the range 150–300 K, a temperature-independent moment $\mu_{eff}\approx 1.3\ \mu_B$. This agrees with measurements made by Miyake *et al.*[4] who reported similar behaviour and a temperature-independent value of $\mu_{eff}\approx 1.1\ \mu_B$. Such a value is compatible with an isolated $U^V(f^1)$ species present in a predominantly axial environment.[18] For a Nb^{IV} (d^1) species, in a low symmetry environment, a temperature-independent 'spin only' value of $\mu_{eff}\approx 1.7\ \mu_B$ would be anticipated. Alternatively, if the d^1 species were sited in an octahedral environment (in a ^2T state) a temperature-dependent moment would be expected. Neither situation corresponds to the observed magnetic behaviour.

Table 12 Observed changes in U—O bond lengths with varying *x* for $UTi_xNb_{3-x}O_{10}$ (values in parentheses are those obtained by Chevalier and Gasperin[2,3])

bond length/Å	UNb_3O_{10}	$UTi_{1/3}Nb_{8/3}O_{10}$	$UTiNb_2O_{10}$
mean $U-O_{ax}$	1.88 (1.95)	1.86 (1.79)	1.79
mean $U-O_{eq}$	2.59 (2.47)	2.57 (2.39)	2.53
v_U	4.7	5.2	6.1

The main conclusions concerning the $UTi_xNb_{3-x}O_{10}$ phases arising from the new structural data are thus: (*a*) the electronic structure of the unsubstituted oxide is $U^VNb^V{}_3O_{10}$; (*b*) in the isostructural series, $UTi_xNb_{3-x}O_{10}$, Ti^{IV} ($r=0.61$ Å) replaces Nb^V ($r=0.64$ Å) by random substitution at both Nb_1 and Nb_2 sites; (*c*) Associated with this substitution is the removal of electrons from uranium according to

$$TiO_2(s)+1/2O_2(g)\xrightarrow{UNb_3O_{10}} Ti_{Nb}{}'+3O_O+h_U{}^{\bullet}$$

where $h_U{}^{\bullet}$ represents the formation of U^{VI} at a U^V site.

$Li_{0.9}UTiNb_2O_{10}$

The framework of the parent oxide is largely undisturbed by the intercalation of lithium (at this degree of insertion) though the mean $U-O_{ax}$ distance increases from its typical 'uranyl' (U^{VI}) value of 1.788 Å in $UTiNb_2O_{10}$ to 1.945 Å in $Li_{0.9}UTiNb_2O_{10}$ in response to electron transfer from lithium to uranium. In the structure of $Li_{0.9}UTiNb_2O_{10}$, shown in Fig. 6, lithium is distributed randomly over the 32h interlayer sites which provide a local five-fold, approximately trigonal bipyramidal, coordination by oxygen about lithium. A similar coordination geometry was found by Dickens and Powell[19] for a lithium intercalation compound of the pillared-layer type oxide α-U_3O_8, $Li_{0.88}U_3O_8$, and the lithium environments in the two compounds are compared in Fig. 7. Bond-valence sums calculated for lithium on the basis of the bond lengths shown in Fig. 7 give a value of *ca.* 1.0, as expected for an intercalated lithium ion.

As the data given in Fig. 4 and Table 11 show, the magnetic susceptibility of the compounds $Li_yUTiNb_2O_{10}$ increases with *y* from the effectively non-magnetic state of $UTiNb_2O_{10}$ to paramagnetic states where the magnetic moment per mole of inserted lithium is *ca.* 1.1–1.3 μ_B. This value approximately equals that found for U^V in the same environment in UNb_3O_{10}. This provides clear evidence that the intercalation process is accompanied by electron transfer, such as has been demonstrated for other U^{VI} compounds,[20] $Li=Li_i{}^{\bullet}+e_U{}'$, where $Li_i{}^{\bullet}$

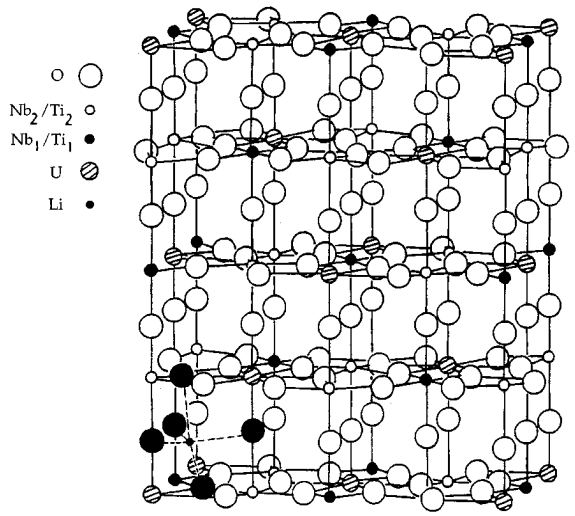

Fig. 6 Occupied lithium site in $Li_{0.9}UTiNb_2O_{10}$, oxygen coordination sphere is highlighted

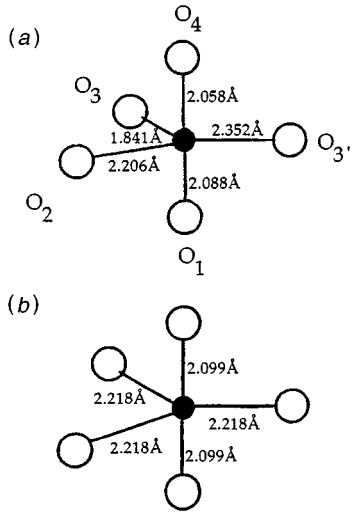

Fig. 7 Comparison of lithium coordination in (*a*) $Li_{0.9}UTiNb_2O_{10}$ and (*b*) $Li_{0.9}U_3O_8$

represents an intercalated cation and $e_{U'}$ an electron trapped at a U^{VI} site. $UTiNb_2O_{10}$ in its intercalation chemistry behaves as a typical framework-type host where intercalation causes marked changes in electronic properties, due to facile reduction of U^{VI}, but only minimal structural change occurs since no interlayer bonds are broken. In this respect it resembles $UTiO_5$ [18] and α-U_3O_8.[19] The facility to alter the U^V to U^{VI} ratio easily and systematically by means of lithium insertion in compounds of this type could be found useful in modifying catalytic activities. Some decrease in the U^V to U^{VI} ratio in the closely related family of compounds $USb_{3-x}Ti_xO_{9-10}$ by substitution of Ti^{IV} for Sb^V in USb_3O_{10} was shown[21] to lead to greatly increased catalytic activity for the ammoxidation of propylene to acrylonitrile.

G.P.S. thanks AEA technology, Harwell, for a studentship and S.P. thanks the Turkish Government for financial assistance.

References

1 A. M. Chippindale, S. J. Crennell and P. G. Dickens, *J. Mater. Chem.*, 1993, **3**, 33.
2 R. Chevalier and M. Gasperin, *C.R. Acad. Sci. Paris, Ser. C*, 1968, **267**, 481.
3 R. Chevalier and M. Gasperin, *C.R. Acad. Sci. Paris, Ser. C*, 1969, **268**, 1969.
4 C. Miyake, S. Ohana, S. Imoto and K. Taniguchi, *Inorg. Chim. Acta*, 1987, **140**, 133.
5 O. Kubaschewski and C. B. Alcock, *Metallurgical Thermochemistry*, Pergamon Press, Oxford, 1979, 5th edn.
6 E. H. P. Cordfunke, R. J. M. Konings, G. Prins, P. E. Potter and M. H. Rand, *Thermochemical Data for Reactor Materials and Fission Products*, AERE, Harwell, UK, 1988.
7 A. M. Chippindale, P. G. Dickens and A. V. Powell, *Prog. Solid State Chem.*, 1991, **21**, 133.
8 G. W. Watt, S. L. Achorn and J. L. Marley, *J. Am. Chem. Soc.*, 1950, **72**, 3341.
9 P. G. Dickens, S. D. Lawrence and M. T. Weller, *Mater. Res. Bull.*, 1985, **20**, 635.
10 ASTM powder diffraction file, 19–859.
11 L. M. Kovba, E. I. Sirotkina and V. K. Trunov, *Zh. Neorg. Khim. (Engl. Transl.)*, 1965, **10**, 188.
12 P. G. Dickens, A. V. Powell and A. M. Chippindale, *Solid State Ionics*, 1988, **28–30**, 1123.
13 D. E. Cox, B. H. Toby and P. Zolliker, Program PROFPV (Brookhaven National Labs./Union Carbide), Oxford VAX version, July 1988.
14 P. G. Dickens and G. P. Stuttard, *J. Mater. Chem.*, 1992, **2**, 691.
15 A. M. Chippindale, P. G. Dickens, G. J. Flynn and G. P. Stuttard, *J. Mater. Chem.*, 1995, **5**, 141.
16 W. I. F. David, R. M. Ibberson and J. C. Matthewman, Profile Analysis of Neutron Powder Diffraction Data at ISIS, Rutherford Appleton Laboratory Report RAL-92-032, 1992.
17 D. Altermatt and I. D. Brown, *Acta Crystallogr., Sect. B*, 1985, **41**, 240.
18 P. G. Dickens, G. P. Stuttard, R. E. Dueber, M. J. Woodall and S. Patat, *Solid State Ionics*, 1993, **63–65**, 417.
19 P. G. Dickens and A. V. Powell, *J. Solid State Chem.*, 1991, **92**, 159.
20 R. E. Dueber, S. Patat and P. G. Dickens, *Solid State Ionics*, 1995, **80**, 231.
21 R. A. Innes, A. J. Perrotta and H. E. Swift, *ACS Symp. Ser.*, 1985, **279**, 75.

Paper 6/05883C; *Received* 27*th August*, 1996